

CORROSION EFFECTS ON THE BUCKLING OF STEEL TANKS UNDER SEISMIC LOADING

Mahmoud R. Maheri & A. Abdollahi
Shiraz University, Iran



SUMMARY

A numerical program is carried out to investigate the effects of internal shell corrosion on the dynamic buckling of three cone roof ground-based, steel cylindrical tanks having different height/diameter ratios subjected to horizontal seismic base excitations. Detailed numerical models of the tank-liquid systems at different stages of corrosion degradation are subjected to two representing accelerograms and for each model the critical peak ground acceleration (PGA) for dynamic buckling of the shell and its associated mode of failure are evaluated. It is found that in all three tanks, the critical PGA is markedly reduced with thinning of the shell, irrespective of the type of ground input. The effects of corrosion degradation on the critical buckling load of the tanks was found to be such that after 20 years of thinning due to corrosion, the static loading alone was responsible for the elephant foot buckling of the shell.

Keywords: steel storage tanks, corrosion, buckling, seismic response, hydrodynamic effects

1. INTRODUCTION

The long-term effect of corrosion in steel liquid storage tank is a significant thinning of the wall section, particularly at lower levels; resulting in imperfections in the shell. The service life of storage tanks is generally planned to be in the range of 20 to 40 years. However, failures of some storage tanks caused by corrosion are reported to have happened after only 1.5 to 2.5 years in service [1]. The American Petroleum Institute states that; approximately 20% of hydrocarbon products lost as leakage are caused by corrosion damage in storage tanks [2]. Corroded steel tanks are particularly susceptible to seismic loading as the imperfections caused by the corrosion highly amplify the seismic response. Corrosion in storage tanks occurs mainly due to the presence of well water, water condensate, atmospheric oxygen and acid gases inside the tank. The atmospheric corrosion of the tank from outside is reported to be of less significance [3]. Oil-derivative sediments containing hydrogen sulfide add to the local acidification of the environment. As a result of the above factors, the sections of the shell most susceptible to corrosion are the lower and the upper parts of the tank wall. Therefore, regarding the state of corrosion, the wall of the tank may be divided into three distinct zones; zone (I) corresponding to the upper part of the wall, which, considering the change in liquid level, may not be in permanent contact with oil and is likely to corrode due to water condensate, atmospheric oxygen and acid gases; zone (II) corresponding to the middle part of the wall which as it is in permanent contact with oil is not susceptible to corrosion and zone (III) represents the lower part of the wall which due to residual water is likely to suffer the most from corrosion. The rate of corrosion in Zone (I) is reported to be around 0.4mm/yr, whereas, that in zone (III) averages around 0.5mm/yr [1].

Little is reported on the effects of corrosion on the dynamic and seismic response of steel storage tanks. The effects of corrosion on the uplift capacity of bottom annular plate of storage tanks subjected to seismic loading [4], as well as, the stability loss due to corrosion of thin-shell cylindrical tanks [5, 6] have been investigated. In a recent work, Dehghan-Manshadi and Maheri [7] also investigated the effects of imperfections due to long term corrosion on the linear dynamic characteristics of steel cylindrical storage tanks. They found that progressive corrosion has significant effects on the tank fundamental period and its associated mode shape of vibration, as well as, the magnitude and location of the maximum hydrodynamic pressures exerted on the tank.

The buckling modes of ground-based cylindrical steel tanks under seismic loading are generally of two forms; (i) elephant foot buckling, characterized by outward bulging of the shell above the base and (ii) diamond shaped buckling, generally occurring at either the lower or the upper sections of the shell [8, 9]. The former type of buckling is of an elasto-plastic nature, whereas, the latter is generally elastic [10]. Natsiavas and Babcock studied the buckling modes of an open-top tall tank subjected to horizontal harmonic base excitation [11]. Experimental studies on tall tanks with roofs were conducted by Nagashima et al [12]. They considered both horizontal and vertical harmonic base excitations. Later, Morita et al. [13] used simulated earthquake excitations to study the buckling behaviour of tanks having height to diameter ratios of 1.2 and 1.3. They showed that the buckling of the shell at the top of the tank, previously considered to be due to the convective component of the liquid hydrodynamic pressure, was indeed caused mainly by the impulsive hydrodynamic pressures. In a later study, Virella et al. [14] investigated the earthquake-induced buckling of steel cylindrical tanks having varying shell thickness. They considered three cone roof tanks having height to diameter ratios (H/D) of 0.40, 0.63 and 0.95 and a constant liquid level of 90% of the height of the tank. They subjected the tanks to two recorded accelerograms and estimated the critical horizontal peak ground acceleration (PGA), causing elastic buckling at the top of the shell. They found that for the taller tanks, the elastic buckling at the top of the shell preceded the plasticity of the shell, regardless of the type of earthquake record considered, whereas, for the shorter tank, depending on the acceleration record considered, plasticity occurred prior to the buckling at the top [14].

In this paper, the effects of long-term corrosion on the buckling response of liquid storage tanks subjected to horizontal ground excitation are investigated. The three tank models considered in [7] and [14] are utilized to investigate the effects.

2. NUMERICAL MODELS OF THE TANKS

The tanks concerned are clamped at base and have cone roofs supported by a number of radial beams and columns. Since only anchored tanks are considered, the bottom of the tank is not included in the model. The first tank, designated Model A, and also referred to as the short tank, has a height to diameter ratio, H/D of 0.40. The second tank (Model B) has an H/D of 0.63 and is also referred to as the medium height tank. The third tank (Model C), referred to as the tall tank has an H/D of 0.95. Fig. 1 shows the geometries of the three tanks. Similar to previous studies, in all the models, the tank was assumed to contain liquid to a level of 90% of the height of the tank wall.

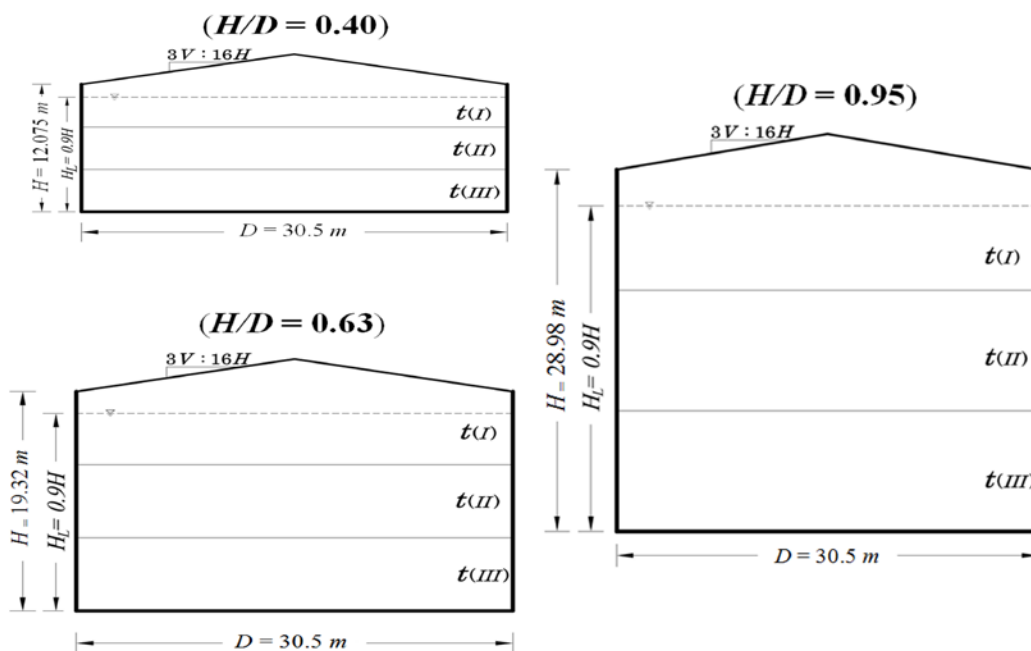


Figure 1. Geometries of the tanks considered [7]

To model the dynamic effects of liquid on the shell the classic added-mass approach is used. This approach is much simpler than the more rigorous Eulerian and Lagrangian approaches; it is supported by most codes of practice [9, 15] and is shown to provide good practical solutions, particularly for short tanks (tanks of low H/D ratios) [16]. In this method, the effective mass of fluid is obtained from a pressure distribution for the impulsive rigid-body mode of the tank-liquid system [17]. Attempts have been made to improve on the classic added-mass solution by including the effects of flexible modes of the tank [18, 19].

In their modeling of the Model-A tank under consideration, Dehghan-Manshadi and Maheri [7] used the ANSYS software to explicitly model the fluid domain and to carry out a Lagrangian solution. They compared their result for the fundamental mode of the tank-fluid system with that of Virella et al. which had used the ABAQUS software and the classic added-mass solution and found that they are almost identical. Taking into consideration the above discussion, and in order that the results may be comparable with those of Virella et al. [14], in the present study, ABAQUS analysis package is utilized to carry out the same added-mass solution of the tank-fluid system as that used in [14]. Similar to [14] for the finite element idealization of the tanks, four-sided doubly-curved shell elements (S4R) are used to model the wall of the tank, three-sided shell elements (S3R) are utilized to model the roof and classic 3D beam elements (B31) are used to model the rafters and columns. Also, crude oil is used in the computations with a density $\rho = 860 \text{ kg/m}^3$ and a bulk modulus $K = 1.65 \text{ GPa}$. Also, the time-dependant effect of corrosion is considered as a constant thinning of the upper third and lower third of the wall height at a rate of 0.4mm/yr and 0.5mm/yr, respectively. For the two tanks with aspect ratios of 0.63 and 0.95 (Models B and C), different shell thickness configurations, corresponding to; as-new and 5 years, 10 years, 15 years, 20 years and 25 years of thinning, are investigated. For the tank model with $H/D = 0.4$ (Model A), due to its small wall thickness, only up to 15 years of corrosion is considered. Details of the sixteen tank models thus created are given in Table 1. The FE mesh of the medium height tank (model B) is shown in Fig. 2.

Table 1. Geometric properties of the steel tanks

Model	Age (years)	H/D	Thickness of central part (mm)	Thickness of the upper and lower parts (mm)
A00	0	0.4	10.2	10.2
A05	5		10.2	7.7
A10	10		10.2	5.2
A15	15		10.2	2.7
B00	0	0.63	16.0	16.0
B05	5		16.0	13.5
B10	10		16.0	11.0
B15	15		16.0	8.5
B20	20		16.0	6.0
C00	0	0.95	21.4	21.4
C05	5		21.4	18.9
C10	10		21.4	16.4
C15	15		21.4	13.9
C20	20		21.4	11.4
C25	25		21.4	8.9

To investigate the dynamic buckling of as-new tapered tanks, two accelerograms recorded during the El Salvador earthquake of 1986 and Parkfield earthquake of 1966 are considered. Descriptions of the selected accelerograms are given in [14]. Also, viscose mass damping for each model is evaluated based on the fundamental period of vibration of the model given in the above reference and for a damping ratio of 2%.

To evaluate the dynamic buckling load of structures the criterion used most extensively was first introduced by Budiansky and Roth [20]. Significant studies using this criterion are due to Babcock et al. [21] and Tanami et al. [22]. Based on this criterion, the structure is subjected to different levels of loading and the load at which there is a significant jump in the response for a small load increment is considered as the critical buckling load. This load signifies the passing of the structure from a stable state into a critical state. The same criterion is used for seismic stability analyses, though in such analyses, due to the high frequency

cyclic nature of loading by which the direction of loading changes suddenly, it is sometimes difficult to identify the occurrence of buckling [14]. The same criterion is used in this study to evaluate the critical buckling load for the tank models.

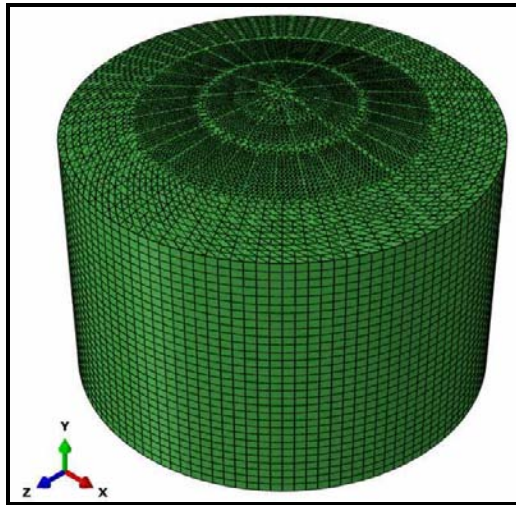


Figure 2. The FE idealization of the tank Model B

3. CORROSION EFFECTS ON BUCKLING OF THE TANKS

To evaluate the critical buckling load for each tank model based on the Budiansky and Roth criterion, the selected accelerograms were scaled to have PGAs ranging from 0.1g to 0.45g. Prior to and during the application of seismic load, each model was subjected to relevant static loads including self weight and hydrostatic load. The results for the three tanks follow.

3.1. Short Tank Model A (H/D = 0.40)

Models relating to this tank included as-new (A-00), and after 5 years (A-05), 10 years (A-10) and 15 years (A-15) corrosion degradation. To determine the critical PGA for each model, the time history responses of the buckling node at different PGAs are plotted and the displacement jump for buckling criteria is located. As an example, such a plot for the tank after 5 years (A-05) subjected to the Parkfield accelerogram is shown in Fig. 3. It can be seen in this figure that the displacement jump occurs at a PGA = 0.25g. Therefore, this level of loading is considered as the critical PGA.

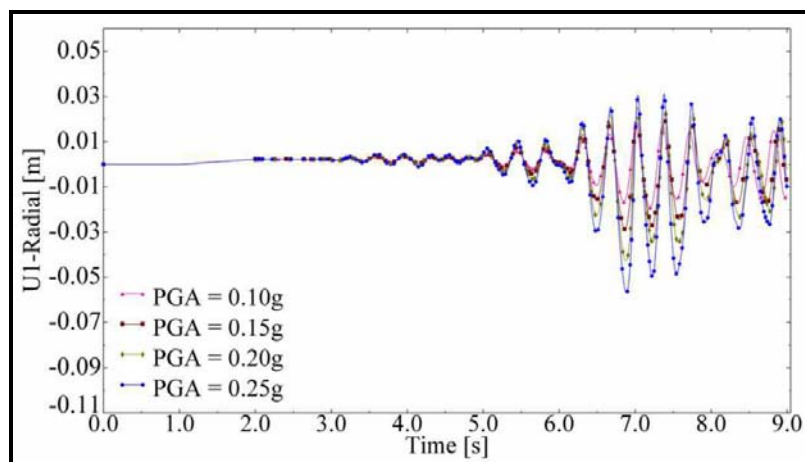


Figure 3. The time history response of the critical node of model A05 at different PGAs of Parkfield record

In Fig. 4 the radial displacement peaks of the buckling node at different levels of loading (PGA) for short tank are plotted. This plot, termed ‘pseudo equilibrium path’ in reference [14], provides useful comparative

view of the corrosion effects on the response of the tank to Parkfield accelerograms. The pseudo equilibrium path for each model shows two distinct parts, signifying different responses. At smaller displacements the curve follows an initially stable path with the slope corresponding to the initial stiffness of the tank. At higher PGAs the slope is reduced indicating an unstable state. The two distinct parts of the curve are idealized by line segments to form a bilinear idealization of the pseudo equilibrium path. The point of intersection of the two lines in the bilinear representation corresponds to the critical PGA. The critical PGAs and the type of buckling failures for this tank subjected to the two earthquake records at different ages are compared in Table 2.

Fig. 4 shows that as the wall thickness reduces with age, the displacements due to static loading increase. The static displacements increase progressively with aging; the increase in the static response of the tank after 5 years being small compared to that after 10 years. The static response after 10 years is equivalent to the as-new tank being subjected to a PGA of around 0.3g. The small change in the critical PGA of the as-new tank (0.25g) and the tank after 5 years (0.23g) indicates that little is changed in that time. However, after 10 years the critical PGA has considerably reduced to 0.1g. The detrimental change in the response of the tank after 10 years can also be deduced when we look at the failure modes of the A05 and A10 models. These failure modes are shown respectively in Fig. 5(a) and Fig. 5(b). The buckling failure of the tank at 5 years is similar to that of the new tank and is in the form of diamond type buckling at the upper part of the tank, whereas, the buckling failure in the tank after 10 years is of the elephant foot nature at the base of the tank. The effects of static loading on this tank were such that the model A15 buckled before it was subjected to seismic base excitation.

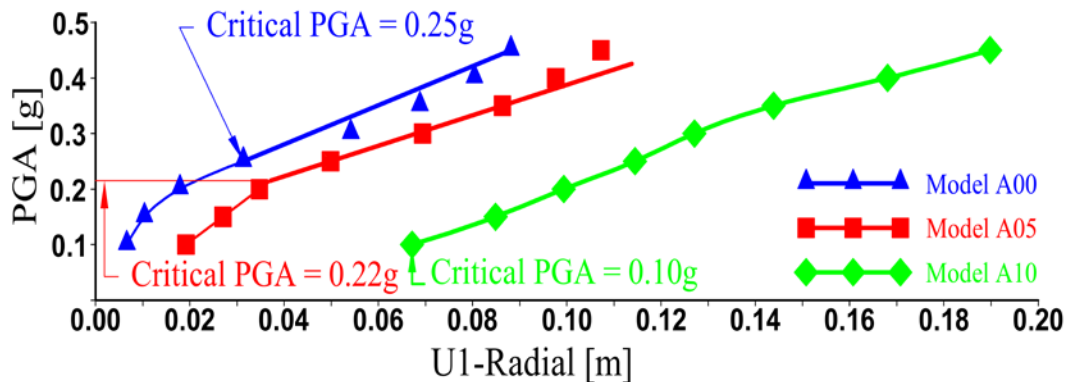


Figure 4. The pseudo equilibrium paths for the critical node of the tank model A subjected to the Parkfield accelerogram.

Table 2. The critical PGA and the buckling mode of different tank models

Model	Age (years)	H/D	Earthquake Accelerogram					
			Parkfield			El Salvador		
			Critical PGA (g)	Buckling Mode	Type of Buckling	Critical PGA (g)	Buckling Mode	Type of Buckling
A00	0	0.4	0.25	Diamond	Elastic	0.277	Diamond	Elastic
A05	5		0.22	Diamond	Elastic	0.21	Diamond	Elastic
A10	10		0.10	EF	Plastic	0.10	EF	Plastic
A15	15		-	EF (Static)	Plastic	-	EF (Static)	Plastic
B00	0	0.63	0.23	Diamond	Elastic	0.26	Diamond	Elastic
B05	5		0.21	Diamond	Elastic	0.20	Diamond	Elastic
B10	10		0.15	Diamond	Elastic	0.19	Diamond	Elastic
B15	15		0.10	EF	Plastic	0.10	EF	Plastic
B20	20		-	EF	Plastic	-	EF	Plastic
C00	0	0.95	0.25	Diamond	Plastic	0.33	Diamond	Elastic
C05	5		0.245	Diamond	Plastic	0.29	Diamond	Elastic
C10	10		0.15	Diamond	Elastic	0.20	Diamond	Elastic
C15	15		0.10	Diamond	Elastic	0.10	EF	Plastic
C20	20		-	EF	Plastic	-	EF	Plastic
C25	25		-	EF (Static)	Plastic	-	EF (Static)	Plastic

The pseudo equilibrium paths for the critical node of this tank at different ages subjected to El Salvador accelerogram, also show similar behaviour under this earthquake; the 5-year old model, with a critical PGA of 0.25g, showing little change in response compared to the as-new tank (critical PGA=0.275g), while the 10-year old model buckles under the combined action of static loading and seismic loading of only PGA=0.1g. Similar observations were reported by Dehghan-Manshadi and Maheri [7] on the dynamic mode shapes and hydrodynamic pressure distribution and amplitudes of the same tank; showing 10 years of degradation being far more detrimental compared to only 5 years of degradation.

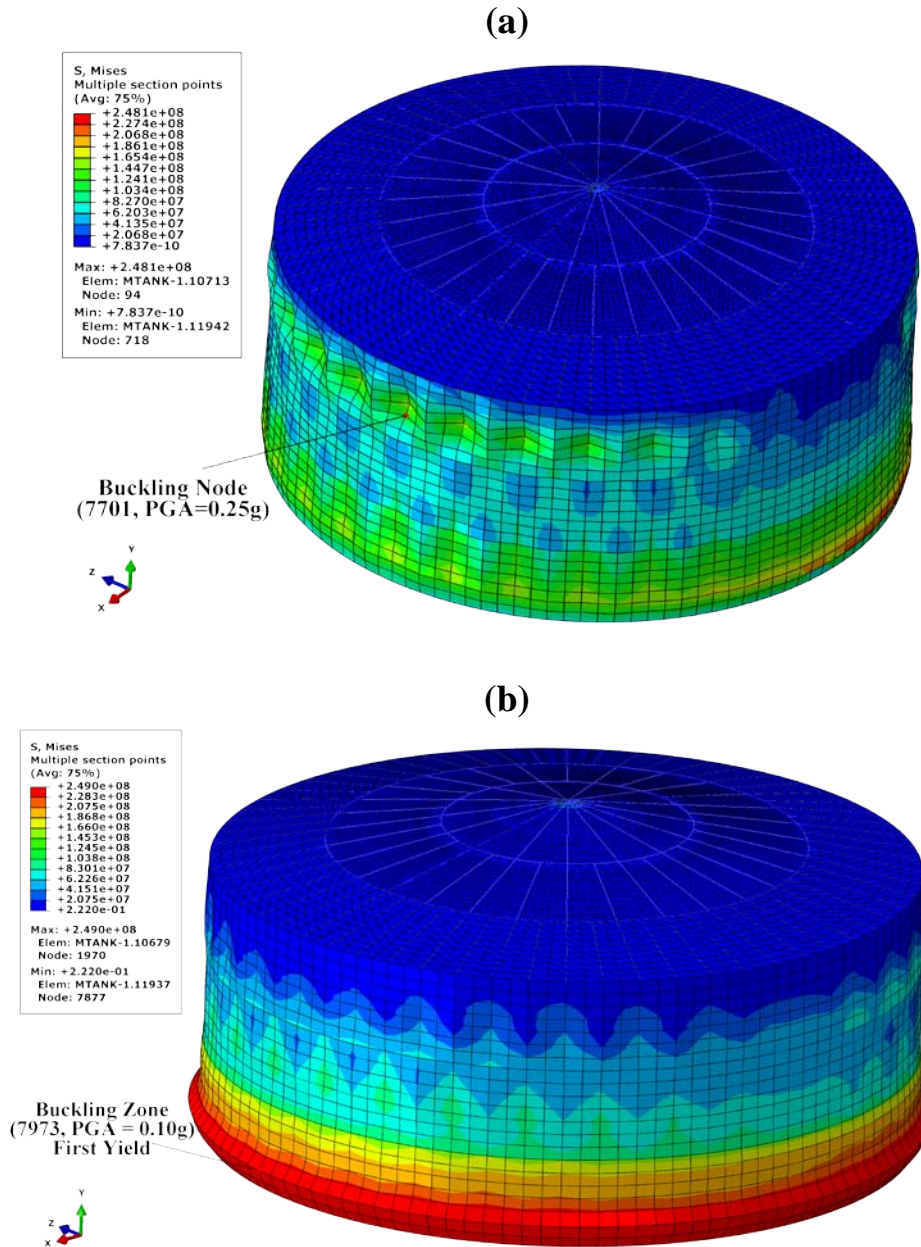


Figure 5. The buckling mode of failure of the short tank (Model A) subjected to Parkfield accelerogram (a) after 5 years and (b) after 10 years of corrosion degradation

3.2. Medium Tank Model B (H/D = 0.63)

The buckling failure of this tank prior to corrosion under the Parkfield and the El Salvador accelerograms is also of a diamond type nature at the upper part of the shell; happening at a critical PGA=0.23g under the Parkfield record and PGA= 0.26g under the El Salvador record (Table 2). After 5 years of corrosion degradation of the shell thickness, the buckling mode of failure due to both accelerograms is unchanged; only the failure happening at reduced PGAs of 0.21g and 0.20g, respectively for the Parkfield and the EL

Salvador records. The time history responses of the buckling node at different PGAs of the San Salvador record for this tank, indicating the displacement jump for buckling criteria are shown in Fig. 6. Contrary to the case of shorter tank (Model A), the buckling failure mode of this tank after 10 years remains unchanged; occurring at a PGA of 0.15g for the Parkfield record and a PGA of 0.19g for the El Salvador record. After 15 years of degradation, however, the dynamic buckling response of the tank to both the Parkfield and the El Salvador accelerograms changes to an elephant foot type occurring at the base of the tank and at a reduced PGA=0.10g in both cases. After 20 years of corrosion degradation, the tank failed in the form of elephant foot buckling prior to seismic base excitation and only under the applied static loading.

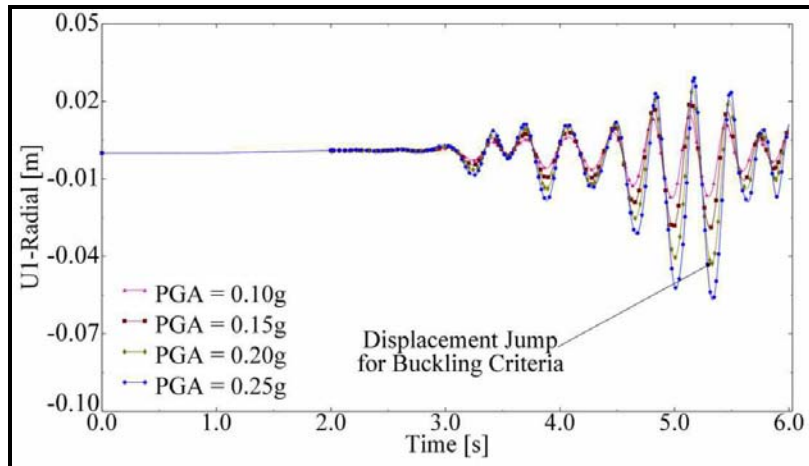


Figure 6. The time history response of the critical node of model B05 at different PGAs of San Salvador record

Fig. 7 shows the pseudo equilibrium paths for this tank at different stages of corrosion degradation and subjected to the Parkfield record. The proximity of the paths for the as-new tank and the tank after 5 years and 10 years of degradation indicates similar dynamic buckling responses (diamond shape). Significant departure of the pseudo equilibrium path for the tank after 15 years away from the other ages signifies the effects of excessive thinning of the shell, resulting in the prominence of the static load effects.

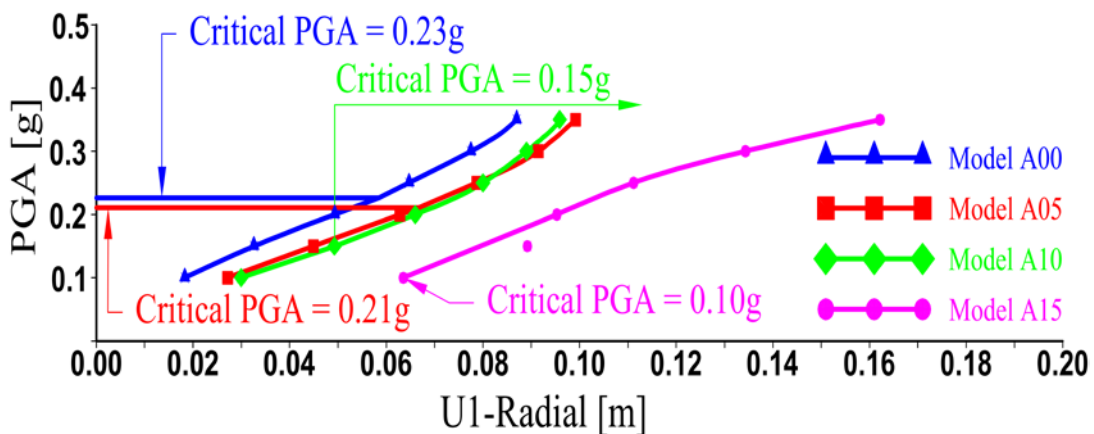


Figure 7. The pseudo equilibrium paths for the critical node of the tank model B subjected to the Parkfield accelerogram.

3.3. Tall Tank Model C (H/D = 0.95)

The buckling failure mode of this tank under both the Parkfield record and the El Salvador record at the states of: as-new, 5 years degradation and 10 years degradation is elastic diamond shape occurring at the upper part of the tank. The tank after 10 years and subjected to the Parkfield record also shows some plastic yielding at the base. The critical PGAs for this tank subjected to the two earthquake records at different ages are compared in Table 2. Also, the time history responses of the buckling node at different PGAs of the Parkfield record for this tank, indicating the displacement jump for buckling criteria are shown in Fig. 8. In this tank, similar to the tank Model B, the change from the diamond-shaped buckling mode to the elephant

foot buckling mode occurs after 15 years of corrosion thinning. This is true when the tank is subjected to either earthquake records. Similar to tank Model B, after 20 years of corrosion degradation, this tank also buckled in an elephant foot form prior to seismic base excitation and only under the applied static loading.

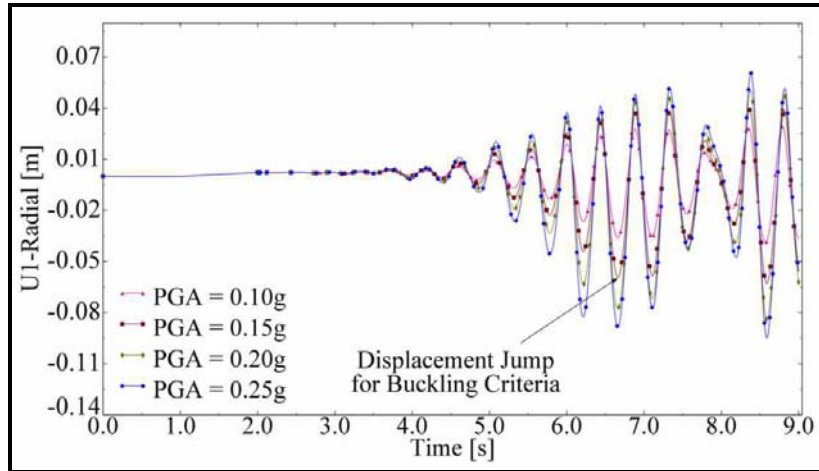


Figure 8. The time history response of the critical node of model C10 at different PGAs of Parkfield record

Fig. 9 shows the pseudo equilibrium paths for this tank at different stages of corrosion degradation subjected to the Parkfield record. Comparing the pseudo equilibrium paths shown in Fig. 9 it is evident that the static displacements of the critical node at older models (C10 and C15) are not as prominent as those seen for models A and B. This has resulted in a situation that, under the Parkfield record and for the as-new model (C00) and the C05 and C15 models, the maximum radial displacements of the critical node at the maximum PGA considered (0.45g) to be almost the same. This, however, is not the trend observed when the tank was subjected to the El Salvador record. Under the El Salvador record, the trend of the pseudo equilibrium paths is similar to those of tank models A and B, with the C15 model undergoing large plastic deformations at higher PGAs.

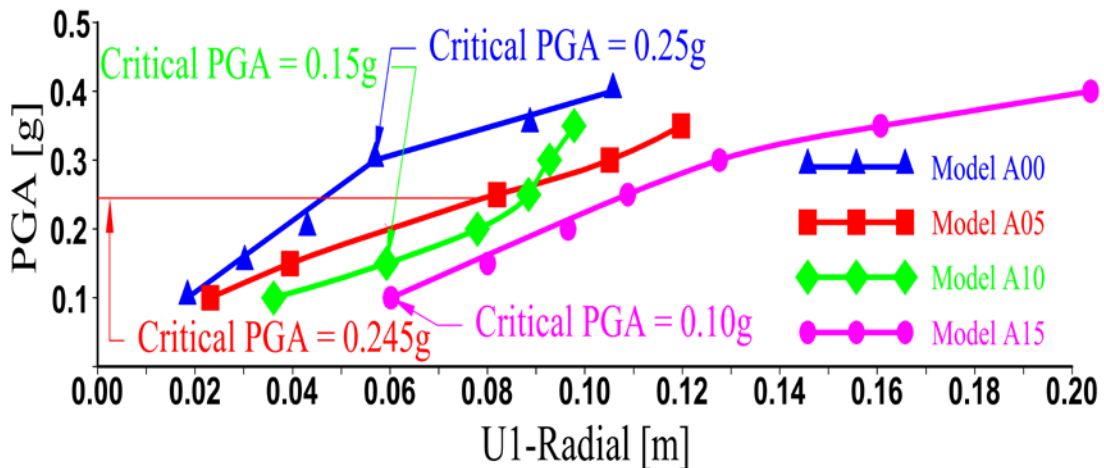


Fig 9. The pseudo equilibrium paths for the critical node of the tank model C subjected to the Parkfield accelerogram.

4. DISCUSSION ON RESULTS

When the effects of corrosion on the short model (Model A) and the medium height model (Model B) are compared, it becomes evident that the change from a diamond shape elastic buckling mode to an elastoplastic elephant foot type buckling mode occurs at a higher age for the taller Model B. It should be noted that this is not so much attributed to the different aspect ratios (L/D) of the tanks, but to the level of thinning of the shell. In Model A, the change in the buckling failure mode to an elephant foot type occurred after 10 years. At this age the thickness of the shell at the lower parts of the tank is reduced to around 50% of its

original thickness. In Model B, however, 10 years degradation results only in about 30% loss of thickness; that is the reason for the change in the buckling mode of failure for this tank at the higher age of 15 years. At this age, Model B tank has similarly thinned at its lower part by around 50%. For the taller tank, model C, the critical thinning ratio appears to be higher. In this tank the elephant foot buckling failure occurred after 15 years of degradation corresponding to a 35% loss of thickness at lower parts.

The ratio of reduced thickness due to corrosion to the original thickness at the lower part of the shell appears to determine the critical change in the buckling mode of failure from an elastic diamond shape to an elasto-plastic elephant foot type. For the short and the medium height tanks under consideration, 50% degradation or thinning appears to be the critical ratio. For the taller tank, the situation is more critical as the critical thinning ratio is increased to 0.65%. It also follows that; the thinning of the shell at the upper part of the tank does not change the buckling mode of failure at that part; the thinning only reduces the critical PGA level at which the diamond-shaped buckling failure occurs. This highlights the fact that corrosion degradation at the bottom section of the tank is more detrimental to its dynamic buckling response compared to degradation at the higher levels. Also, Table 2 shows that for the short tank (Model A), the effects of type of earthquake input on the dynamic buckling mode at different ages and the corresponding critical PGAs, are minimal. The buckling mode of failure under both records is the same at all ages; only the critical PGA for the as-new tank under El Salvador record being slightly higher than that under the Parkfield record. The effects of type of earthquake record on the Model B tank is more or less the same as Model A. However, for the taller tank, (Model C) at different ages, the critical PGAs under the El Salvador record are markedly higher than those for the Parkfield record. The buckling mode of failure of the tank after 15 years subjected to the El Salvador record is of elephant foot type, as opposed to the diamond-shaped failure seen under the Parkfield record.

5. CONCLUSIONS

Comparative evaluations of results, as presented in this paper, indicates that the thinning of the wall of a steel tank due to corrosion has a marked effect on the type of dynamic buckling failure; changing a diamond-shaped buckling failure at the top of the as-new tank to an elephant foot buckling failure at the base. The effects of corrosion degradation of the wall thickness also have considerable effect on the critical peak ground acceleration (PGA) for the formation of the buckling failure. After only 10 years of degradation, critical PGAs have reduced by as much as 175% in the short tank, 53% in the medium height tank and 67% in the tall tank. The effects of corrosion thinning of the wall around the base is such that at the equivalent age of 15 years, and prior to the seismic excitation, the short tank undergoes elephant foot type buckling failure under the static loading due to self weight and hydrostatic pressures. The corresponding age for the medium height and tall tanks is increased to 20 years. The effects of type of earthquake input on the buckling mode for the short tank and the medium height tank appear to be insignificant.

REFERENCES

- [1] Medvedeva, M.L., Tiam, T.D., (1998). Classification of corrosion damage in steel storage tanks, *Chemical and Petroleum Engineering*, 34(9-10).
- [2] American Petroleum Institute, (1988). API Standard 650, Steel tanks for oil storage, 8th ed.
- [3] Zagórski, A., Matysiak, H., Tsyrlunyk, O., Zvirko, O., Nykyforchyn, H., Kurzydłowski, K., (2004). Corrosion and stress-corrosion cracking of exploited storage tank steel, *Material Science*, 40(3).
- [4] Yamaguchi, S., Ishida, K., Ibata, T., Kawano, K., Sekine, K., Maruyama, H., (2006). A study of influence of locally reduced thickness on stress of bottom annular plate of oil storage tank during uplifting by seismic loading, *Proc. ASME PVP Conference on Maintenance and Safe Operation*, 23-27.
- [5] Gutma, E., Haddad, J., Bergman, R., (2000). Stability of thin-walled high-pressure vessels subjected to uniform corrosion, *Thin-Walled Structures*, 38, 43-52.
- [6] Bergman, R.M., Levitsky, S.P., Haddad, J., Gutman, E.M., (2006). Stability loss of thin-walled cylindrical tubes, subjected to longitudinal compressive forces and external corrosion, *Thin-Walled Structures*, 44, 726-729.
- [7] Dehghan-Manshadi, S.H., Maheri, M.R., (2010). The effects of long term corrosion on the dynamic characteristics of ground based cylindrical liquid storage tanks, *Thin-Walled Structures*, 48(12): 888-896.

- [8] Cooper TW, Wachholz TP, (1999). Optimizing post-earthquake lifeline system reliability, Proceedings of the 5th US Conference on Lifeline Earthquake Engineering, ASCE, Vol. 16, p.878-86.
- [9] American Lifelines Alliance, (2001). Seismic fragility formulations for water systems, ASCE, Part-1: Guideline, Part-2: Appendices.
- [10] Handam FH, (2000). Seismic behavior of cylindrical steel storage tanks, Constructional Steel Research, 53:307-333.
- [11] Teng JG, Rotter JM, Buckling of thin metal shells, London: Spon Press, Taylor and Francis; 2004.
- [12] Natsiavas S, Babcock CD, (1987). Buckling at the top of a fluid-filled tank during base excitation, ASME Journal of Pressure Vessel Technology, 109:374-380.
- [13] Nagashima H, Kokubo K, Takayanagi M, Saitoh K, Imaoka T, (1987). Experimental study on the dynamic buckling of cylindrical tanks: Comparison between static buckling and dynamic buckling, JSME, 30(263):737-746.
- [14] Morita H, Ito T, Hamada K, Sugiyama A, Kawamoto Y, Ogo H et al., (2003). Investigation on buckling behavior of liquid storage tanks under seismic excitation, Proceedings of the ASME Pressure Vessels and Piping Conference, Vol. 466, p. 227-234.
- [15] American Water Works Association, (1984). AWWA Standard for welded steel tanks for water storage. AWWA D100.
- [16] Veletsos, A.S., (1984). Seismic response and design of liquid storage tanks; Guidelines for the seismic design of oil and gas pipeline systems, Technical Council on Lifeline Earthquake Engineering. New York; ASCE, 255-37-, 443-461.
- [17] Veletsos A.S., Shivakumar, P., (1997). Tanks containing liquids or solids. In: Beskos DE, Poulos A, ditors. Computer analysis and design of earthquake resistant structures: A Handbook, 3, 725-773 (chapter 15).
- [18] Veletsos A.S., (1974). Seismic effects in flexible liquid storage tanks, Proceedings of the 5th World Conference on Earthquake Engineering, 1, 630-639.
- [19] Maheri M. R., (2002). Solution of structure-fluid dynamic interaction using a modified added-mass approach, Dam Engineering, XIII (1):25-50.
- [20] Budiansky B, Roth S, (1962). Axisymmetric dynamic buckling of clamped shallow spherical shells, NASA collected papers on stability of shell structures, TN-1510, p. 597-606.
- [21] Babcock CD, Baker WE, Fly J, Bennet JG, (1984). Buckling of steel containment shells under time-dependant loading, In: Mechanical/Structural Engineering Branch Division of Engineering Technology, Washington (DC): Office of Nuclear Regulatory Commission.
- [22] Tanami T, Taki S, Hangai Y, (1988). Dynamic buckling of shallow shells under the up-and-down earthquake excitation. Proceedings of the ninth World Conference on Earthquake Engineering, Vol. V, p. 545-50.